Physicochem. Probl. Miner. Process., 58(1), 2022, 169-180

http://www.journalssystem.com/ppmp

Physicochemical Problems of Mineral Processing

ISSN 1643-1049

Received November 24, 2021; reviewed; accepted December 29, 2021

Direct conversion of alkaline earth metal hydroxides and sulfates to carbonates in ammonia solutions

Ilhan Ehsani [1], Arman Ehsani [2], Ayse Ucyildiz [3], Abdullah Obut [3]

[1] Şırnak University, Mining Engineering Department, 73000, Şırnak, Turkey

[2] Adana Alparslan Türkeş Science and Technology University, Mining Engineering Department, 01250, Adana, Turkey

[3] Hacettepe University, Mining Engineering Department, 06800, Ankara, Turkey

Corresponding author: ilhanehsani@sirnak.edu.tr (Ilhan Ehsani)

Abstract: In this study, the direct conversion behaviors of different alkaline earth metal solids (the hydroxides and the sulfates of alkaline earth metals Ca, Sr, Ba and Mg) to their corresponding carbonates in dissolved carbonate-containing pregnant solutions obtained by direct leaching of a smithsonite ($ZnCO_3$) ore sample in aqueous ammonia solutions having different concentrations (4 M, 8 M and 13.3 M NH_3) were investigated by using X-ray diffraction analyses at alkaline earth metal to dissolved carbonate mole ratios of 1:1 and 1:2, for revealing the conversion possibilities of dissolved carbonate in the pregnant solutions to solid carbonate by-products. The results of direct conversion experiments showed that $Ca(OH)_2$, $CaSO_4 \cdot 2H_2O$, $Sr(OH)_2 \cdot 8H_2O$ and $Ba(OH)_2 \cdot 8H_2O$ converted to their corresponding carbonates, $SrSO_4$ partially converted to $SrCO_3$ as observed by the presence of unreacted $SrSO_4$ peaks in X-ray diffraction patterns of the converted solids, and $BaSO_4$ did not convert to $BaCO_3$ because of its lower solubility with respect to $BaCO_3$. On the other hand, it was observed that $Mg(OH)_2$ did not convert to $MgCO_3$, but $MgSO_4 \cdot 7H_2O$ converted dominantly to an uncommon phase, which was tentatively identified as $Mg_5Zn_3(CO_3)_2(OH)_{12} \cdot H_2O$. In the study, a complete discussion on the conversion behaviors of alkaline earth metal solids to their corresponding carbonates was given considering the differences between their solubility product constants and the changes in the free energies of the theoretical conversion reactions. In addition, infrared spectra and scanning electron microscope images of some of the converted solids were also presented for characterization purposes.

Keywords: alkaline earth metal, ammonia leaching, direct conversion, dissolved carbonate, smithsonite

1. Introduction

The hydrometallurgical 'direct conversion' process is one of the two commercial processes used for the production of strontium carbonate ($SrCO_3$), which is utilized mainly in the preparation of ferrite magnets (i.e. $SrFe_{12}O_{19}$), glasses and other strontium chemicals, from celestine (natural $SrSO_4$) ores and concentrates. In the direct conversion process, solid celestine feed is added to a hot (>80°C) aqueous solution of sodium carbonate, which is the source of dissolved carbonate, to obtain solid strontium carbonate product according to Eq. (1). The conversion reaction (Eq. (1)) proceeds to the right (product) side because of the great difference between the solubility product constants of $SrSO_4$ ($K_{sp}=3.44 \cdot 10^{-7}$) and $SrCO_3$ ($K_{sp}=5.60 \cdot 10^{-10}$) and the negative free energy change of Eq. (1) (Carrillo et al., 1995; Castillejos et al., 1996; Lide, 2010; Pullar, 2012; Singerling, 2017). In addition to the conventional direct conversion process, celestine could also be converted to strontium carbonate directly with the use of sodium carbonate by mechanochemical (Obut et al., 2006; Erdemoglu et al., 2007; Setoudeh et al., 2010, Sezer and Arslan, 2019) and hydrothermal (Suarez-Orduna et al., 2004,2007) processes. On the other hand, Yan et al. (2021) used sodium bicarbonate and Bingol et al. (2012), Zoraga and Kahruman (2014), Zoraga et al. (2016), Hizli et al. (2017) and Icin et al. (2021) used ammonium carbonate as the source of carbonate for the conversion of celestine to strontium carbonate.

DOI: 10.37190/ppmp/145415

$$SrSO_{4(s)} + CO_3^{2-}{}_{(aq)} \leftrightarrow SrCO_{3(s)} + SO_4^{2-}{}_{(aq)} \quad (\Delta G^0 = -8.7 \text{ kJ/mol}) \quad (1)$$

Zinc is an industrially important metal with the main use in galvanizing and is extracted primarily from the sulfide (i.e. sphalerite, ZnS) and the non-sulfide (i.e. smithsonite, $ZnCO_3$) zinc ores. For the extraction of zinc from smithsonite ores, the direct (without pre-heating) leaching process in ammonia solutions is widely studied in the literature due to the selectivity of ammonia for smithsonite dissolution against the major gangue minerals (i.e., goethite, calcite and/or dolomite) in these ores (Frenay, 1985; Ding et al., 2013; Li et al., 2018; Ehsani et al., 2021). Following leaching, the dissolved zinc in carbonate-containing ammoniacal pregnant solutions may be recovered in metallic or compound forms (i.e., as $Zn_5(CO_3)_2(OH)_6$) by different processes (Harvey, 2006).

It seems possible that other than the direct use of sodium carbonate or ammonium carbonate chemicals as the source of dissolved carbonate, the dissolved carbonate that formed during hydrometallurgical processing of a carbonate-containing primary source may also be utilized for the direct conversion purpose, as demonstrated by Ehsani and Obut (2019) for the dissolved carbonate-containing pregnant solution formed after sodium hydroxide leaching of a smithsonite ore sample. Therefore, in this study, for the first time, the direct conversion behaviors of different alkaline earth metal hydroxides and sulfates to their corresponding carbonates in dissolved carbonate-containing pregnant solutions obtained by direct leaching of a smithsonite ore sample in aqueous ammonia solutions were systematically investigated by X-ray diffraction (XRD) analyses. For characterization purposes, the attenuated total reflection-infrared (ATR-IR) spectra and the scanning electron microscope (SEM) images of some of the converted solids were also determined.

2. Materials and methods

The hydroxides and the sulfates of some of the alkaline earth metals, namely reagent grade calcium hydroxide ($Ca(OH)_2$), natural calcium sulfate dihydrate (gypsum, $CaSO_4 \cdot 2H_2O$), reagent grade strontium hydroxide octahydrate ($Sr(OH)_2 \cdot 8H_2O$), reagent grade strontium sulfate ($SrSO_4$), natural strontium sulfate (celestine, $SrSO_4$), reagent grade barium hydroxide octahydrate ($Ba(OH)_2 \cdot 8H_2O$), reagent grade barium sulfate ($BaSO_4$), reagent grade magnesium hydroxide ($Mg(OH)_2$) and reagent grade magnesium sulfate heptahydrate ($MgSO_4 \cdot 7H_2O$), were used in the direct conversion experiments as the solid feed materials. Because of the generally observed low solubility product constants of alkaline earth metal carbonates (Table 1), the above-mentioned alkaline earth metal-containing solids were selected and used in the experimental studies.

Table 1. Solubility product constants of selected alkaline earth metal solids (Lide, 2010)

$Mg(OH)_2$	$5.61 \cdot 10^{-12}$	$MgSO_4 \cdot 7H_2O$	freely soluble*	$MgCO_3$	$6.82 \cdot 10^{-6}$
$Ca(OH)_2$	$5.02 \cdot 10^{-6}$	$CaSO_4 \cdot 2H_2O$	$3.14 \cdot 10^{-5}$	$CaCO_3$	$3.36 \cdot 10^{-9}$
$Sr(OH)_2 \cdot 8H_2O$	sparingly soluble*	$SrSO_4$	$3.44 \cdot 10^{-7}$	$SrCO_3$	$5.60 \cdot 10^{-10}$
$Ba(OH)_2 \cdot 8H_2O$	soluble*	$BaSO_4$	$1.08 \cdot 10^{-10}$	$BaCO_3$	$2.58 \cdot 10^{-9}$

*: see text

A representative conversion experiment was initiated by the addition of calculated amounts (according to alkaline earth metal to dissolved carbonate mole ratios of 1:1 and 1:2) of alkaline earth metal solid to a 110 mL dissolved carbonate-containing (the dominant carbon-containing dissolved specie is CO_3^{2-} anion; Carrillo et al., 1995) pregnant solution formed after direct leaching of a local (Kayseri/Turkey) smithsonite ore sample in 4 M, 8 M or 13.3 M NH_3 solution. Henceforward, these solutions were called as 4 M, 8 M and 13.3 M pregnant solution, respectively. The dissolved carbonate contents of the pregnant solutions obtained after leaching in 4 M, 8 M and 13.3 M NH_3 solutions, calculated according to the leaching ratio values of zinc in the ore sample (Ehsani et al., 2021), were 24.2 g/L, 48.6 g/L and 82.8 g/L, respectively. The properties of the smithsonite ore sample, the details of the leaching procedure and conditions, the obtained leaching ratio values and the other properties of pregnant solutions were given in Ehsani et al. (2021). Following a conversion time of two hours under magnetic stirring at room temperature, the converted solid was obtained by centrifugation, water washing and drying at 105°C in a laboratory oven. The alkaline earth metal to dissolved carbonate mole

ratios, the conversion time and the initial ammonia concentrations of solutions used in the leaching were determined according to preliminary experiments and previous literature studies (Ehsani and Obut, 2019; Ehsani et al., 2021). The room temperature was selected as the conversion temperature because of the instabilities of the pregnant solutions at higher temperatures (Harvey, 2006; Ehsani et al., 2021). Finally, the converted solid was stored in covered glass bottles for XRD analysis (Rigaku-Miniflex 600, CuKα radiation). The ATR-IR spectra (Perkin Elmer-Spectrum 2), the SEM images (FEI-Inspect F50) and the thermal analyses (TG/DTA) curves (Setaram-Labsys, heating rate=10°C/minute) of some of the converted solids were also determined for detailed characterization.

3. Results and discussion

Because calcium is the most abundant alkaline earth metal among the investigated metals (order of abundance in the earth's crust: 5, average content in the earth's crust: $4.15 \cdot 10^4$ g/ton; Enghag, 2004), the direct conversion experiments were started with the use and comparison of two different calcium-containing solids. The XRD patterns of $Ca(OH)_2$ and its converted solids (Fig. 1) obtained by direct conversion at $Ca:CO_3^{2-}$ mole ratios of 1:1 and 1:2 in 4 M, 8 M and 13.3 M pregnant solutions indicated that all converted solids obtained in three different pregnant solutions were dominantly calcium carbonate of calcite polymorph. For all of the pregnant solutions studied, the conversion at $Ca:CO_3^{2-}$ mole ratio of 1:2 generally produced purer solids in comparison to the mole ratio of 1:1, for which the converted solids, in addition to the dominant $CaCO_3$ phase, contained low amounts of hydrated calcium hydroxyzincate ($CaZn_2(OH)_6 \cdot 2H_2O$; JCPDS card no: 24-0222) and zinc oxide (ZnO, JCPDS card no: 36-1451) phases. The only single-phase converted solid, whose XRD pattern contained only peaks of $CaCO_3$ (Calcite, JCPDS card no: 5-0586), was obtained at $Ca:CO_3^{2-}$ mole ratio of 1:2 following direct conversion in 4 M pregnant solution. The complete conversion of $Ca(OH)_2$ to $CaCO_3$ was expected due to the great difference between the solubility product constants of $Ca(OH)_2$ and $CaCO_3$ (Table 1) and the negative free energy change (Barin, 1995; Free, 2013) of the related conversion reaction (Eq. (2)).

$$Ca(OH)_{2(s)} + CO_3^{2-}{}_{(aq)} \leftrightarrow CaCO_{3(s)} + 2OH^-{}_{(aq)} \quad (\Delta G^0 = -17.1 \text{ kJ/mol}) \tag{2}$$

It can be seen from Fig. 2 that $CaSO_4 \cdot 2H_2O$ also converted mainly to calcium carbonate of calcite polymorph and the converted solids generally were purer (the only impurity observed was $CaSO_4 \cdot 0.5H_2O$) than the converted solids obtained from $Ca(OH)_2$ under all experimental conditions studied. The conversion could easily be followed by the disappearance of $CaSO_4 \cdot 2H_2O$ peaks, i.e. at 2θ=11.64, 20.74 and 29.12° (Gypsum, JCPDS card n o: 33-0311), and the appearance of newly formed

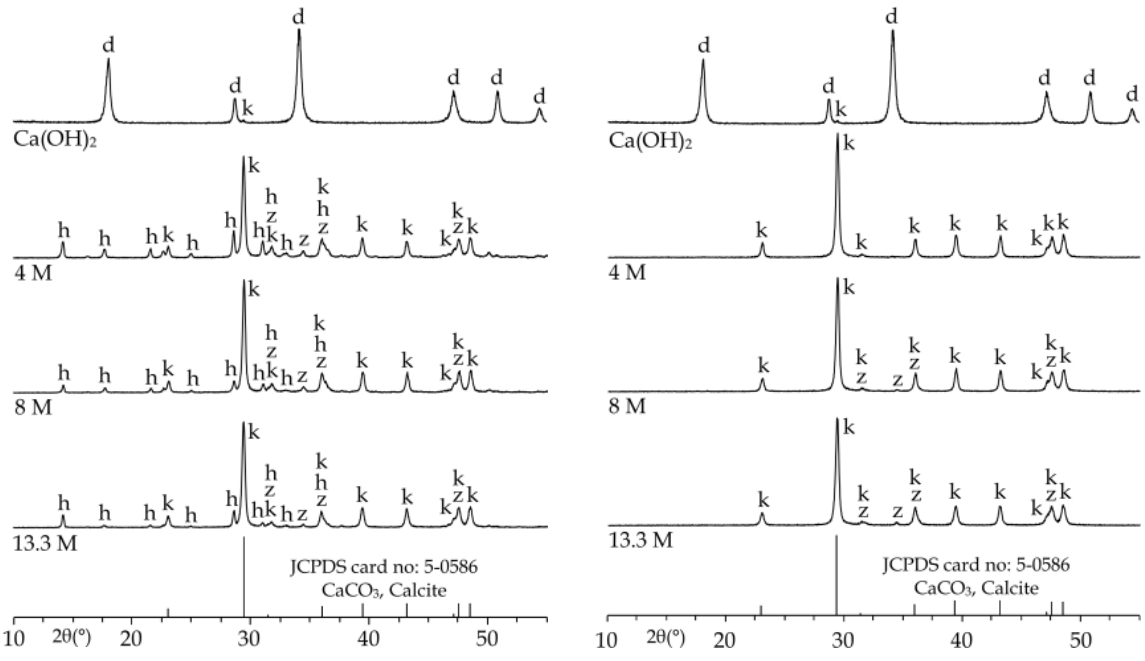

Fig. 1. XRD patterns of $Ca(OH)_2$ and its converted solids obtained after conversion in indicated pregnant solutions ($Ca:CO_3^{2-}$ mole ratios; left 1:1 and right 1:2) (d:$Ca(OH)_2$, h:$CaZn_2(OH)_6 \cdot 2H_2O$, k:$CaCO_3$, z:ZnO)

$CaCO_3$ peaks, i.e. at 2θ=29.43, 39.47 and 43.23°, in XRD patterns of the converted solids. The complete conversion of $CaSO_4 \cdot 2H_2O$ to $CaCO_3$ according to Eq. (3) was expected due to the great difference between the solubility product constants of the feed and the product solids (Table 1), and the negative free energy change (Barin, 1995; Free, 2013) of the conversion reaction. The results of direct conversion experiments using calcium-containing solids indicated that it was possible to integrate naturally abundant gypsum into the processing of smithsonite ores by ammonia leaching for the obtainment of calcium carbonate by-product, which may found use in various industries, e.g. paper, paints, plastics, rubber and others (Phipps, 2014; Thenepalli et al., 2015; Jimoh et al., 2018).

$$CaSO_4 \cdot 2H_2O_{(s)} + CO_3^{2-}{}_{(aq)} \leftrightarrow CaCO_{3(s)} + SO_4^{2-}{}_{(aq)} + 2H_2O_{(l)} \quad (\Delta G^0 = -22.6 \text{ kJ/mol}) \tag{3}$$

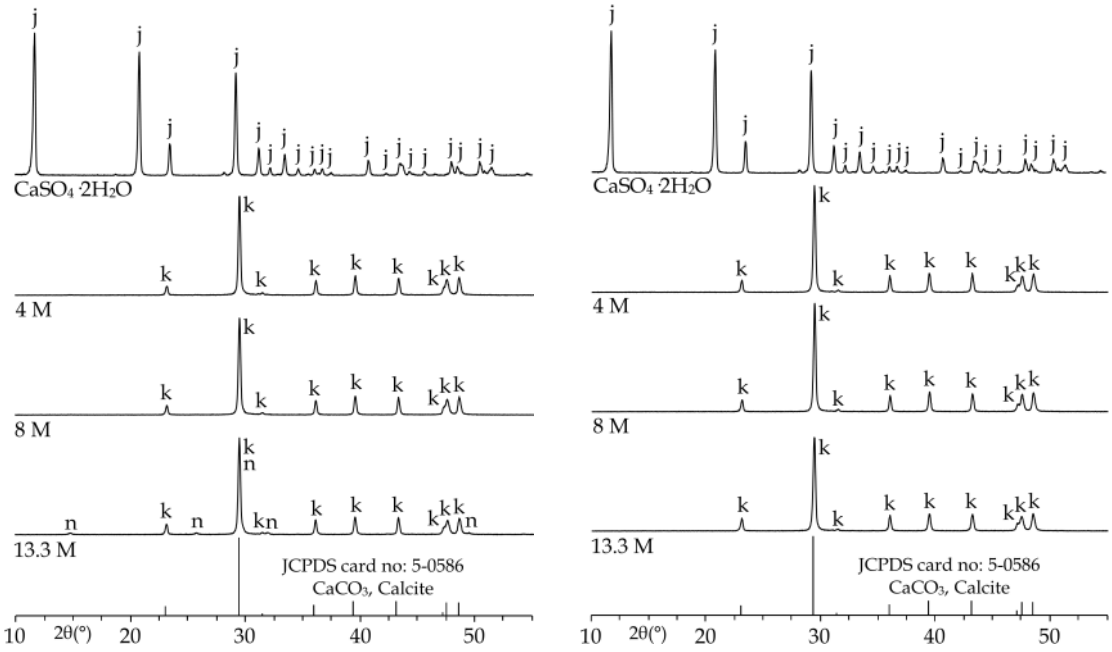

Fig. 2. XRD patterns of $CaSO_4 \cdot 2H_2O$ and its converted solids obtained after conversion in indicated pregnant solutions ($Ca:CO_3^{2-}$ mole ratios; left 1:1 and right 1:2) (j:$CaSO_4 \cdot 2H_2O$, k:$CaCO_3$, n:$CaSO_4 \cdot 0.5H_2O$)

In a previous study, Ehsani and Obut (2019) observed a near-total conversion of gypsum and reagent grade calcium hydroxide to dominantly calcium hydroxyzincate ($CaZn_2(OH)_6 \cdot 2H_2O$) containing solids, in place of $CaCO_3$, probably according to Equation (4) (Wang and Wainwright, 1986; Zhu et al., 2015), in a dissolved carbonate-containing pregnant zinc solution formed after leaching of a smithsonite ore sample in 4 M NaOH solution. In this study, calcium hydroxyzincate phase was observed to form in quite low amounts for only $Ca(OH)_2$ used experiments, possibly due to the existence of dominant zinc ammine ($Zn(NH_3)_4^{2+}$) complex, in place of the zincate ($Zn(OH)_4^{2-}$) complex, in the studied ammoniacal pregnant zinc solutions (Ding et al., 2013). On the other hand, it was observed that the less stable polymorphs, aragonite and vaterite, of calcite did not form under the studied experimental conditions for both of the used calcium-containing solids.

$$Ca(OH)_2 + 2Zn(OH)_4^{2-} + 2H_2O \leftrightarrow CaZn_2(OH)_6 \cdot 2H_2O + 4OH^- \tag{4}$$

For characterization purposes, the particle morphologies of single-phase converted solids obtained from $Ca(OH)_2$ and $CaSO_4 \cdot 2H_2O$ at $Ca:CO_3^{2-}$ mole ratio of 1:2 in 4 M NH_3 pregnant solution were determined by SEM analyses. The SEM images given in Fig. 3 showed that calcium carbonate particles obtained by the conversion of calcium-containing solids generally had a rhombohedral morphology, as also observed for the calcium carbonate precipitates of calcite polymorph in different literature studies (Kralj et al., 2004; Cheng et al., 2014; Liu et al., 2014), but the particles obtained from $Ca(OH)_2$ were more rounded, agglomerated and smaller than the particles obtained from $CaSO_4 \cdot 2H_2O$.

Although strontium is the least abundant alkaline earth metal (order of abundance in the earth's crust: 15, average content in the earth's crust: 370 g/ton; Enghag, 2004) among the investigated metals, the direct conversion experiments continued with strontium containing alkaline earth metal solids due

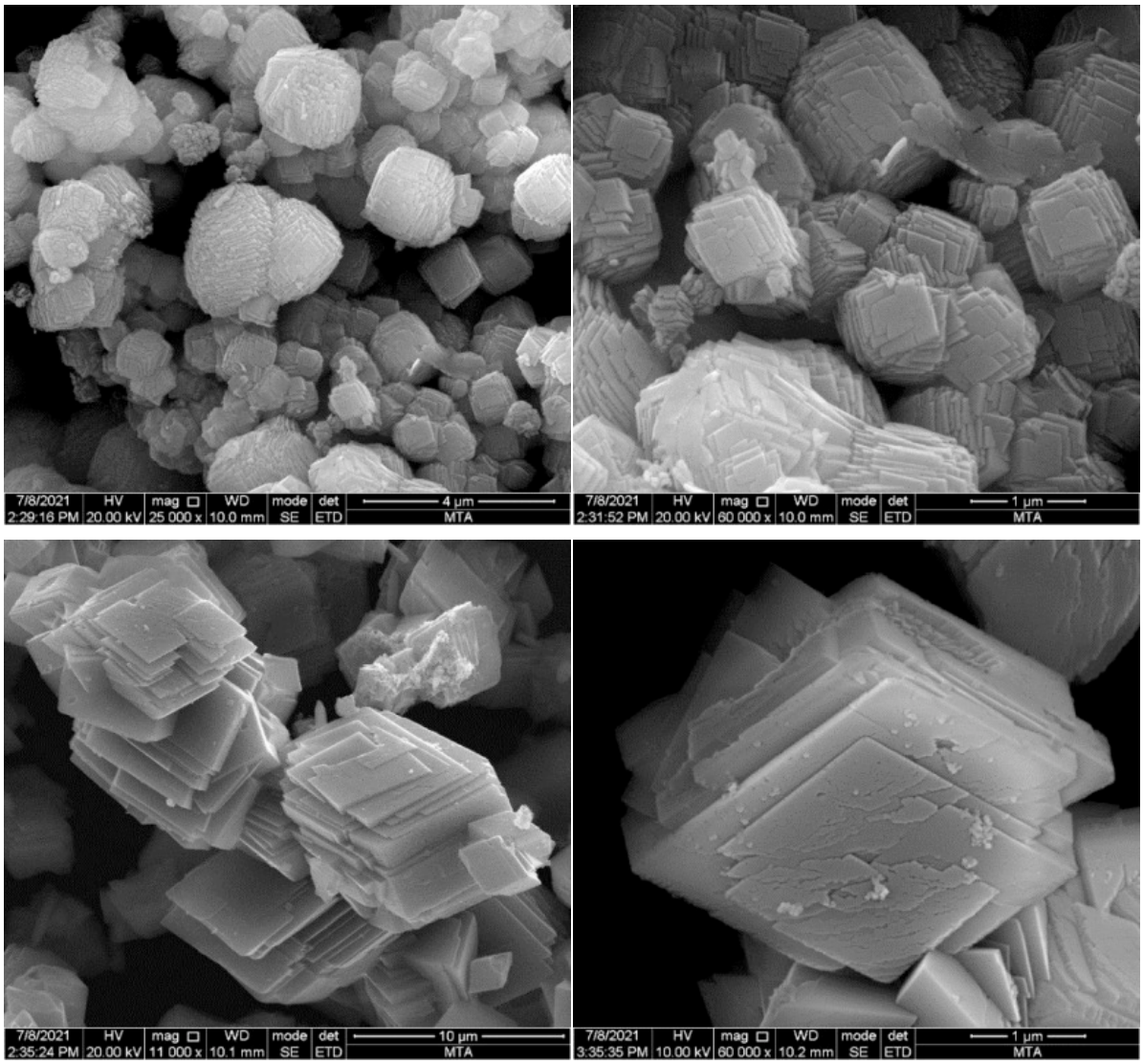

Fig. 3. SEM images of $CaCO_3$ particles obtained by conversion of $Ca(OH)_2$ (top) and $CaSO_4 \cdot 2H_2O$ (bottom)

to the presence of abundant strontium reserves in Turkey (MTA, 2021). The XRD patterns of $Sr(OH)_2 \cdot 8H_2O$ and its converted solids (Fig. 4) obtained by the direct conversion at $Sr:CO_3^{2-}$ mole ratios of 1:1 and 1:2 in 4 M, 8 M and 13.3 M pregnant solutions showed that all converted solids obtained in three different pregnant solutions contained strontium carbonate as the main phase, which was expected due to the great difference between the solubilities of sparingly water-soluble $Sr(OH)_2 \cdot 8H_2O$ ($0.90^{0°C}$ g/100 mL H_2O and $47.7^{100°C}$ g/100 mL H_2O; Patnaik, 2003) and water-insoluble $SrCO_3$ ($0.00034^{20°C}$ g/100 g H_2O; Lide, 2010). The single-phase converted $SrCO_3$ (Strontianite, JCPDS card no: 5-0418), which did not contain any hydroxides of strontium ($Sr(OH)_2$; JCPDS card no: 27-0847 and $Sr(OH)_2 \cdot H_2O$; JCPDS card no: 28-1222) in minor amounts, was only obtained at $Sr:CO_3^{2-}$ mole ratio of 1:2 after direct conversion in 13.3 M pregnant solution.

The SEM image and the ATR-IR spectrum of single-phase converted solid obtained from $Sr(OH)_2 \cdot 8H_2O$ were also determined for characterization purposes. The SEM image (Fig. 5) showed that the shapes of prepared strontium carbonate particles were rod-like, as also found for the strontium carbonates synthesized in the literature studies (Li et al., 2012; Zhang et al., 2017). It could also be seen from Fig. 5 that the converted solid had a very strong adsorption band at 1444 cm^{-1} due to asymmetric stretching, a strong band at 856 cm^{-1} due to out-of-plane bending, and a doublet at 706 and 699 cm^{-1} due to planar bending of carbonate groups in the structure of strontium carbonate. A very weak absorption peak was also observed at 1071 cm^{-1}, which may be attributed to the symmetric stretching of the carbonate groups (Adler and Kerr, 1963).

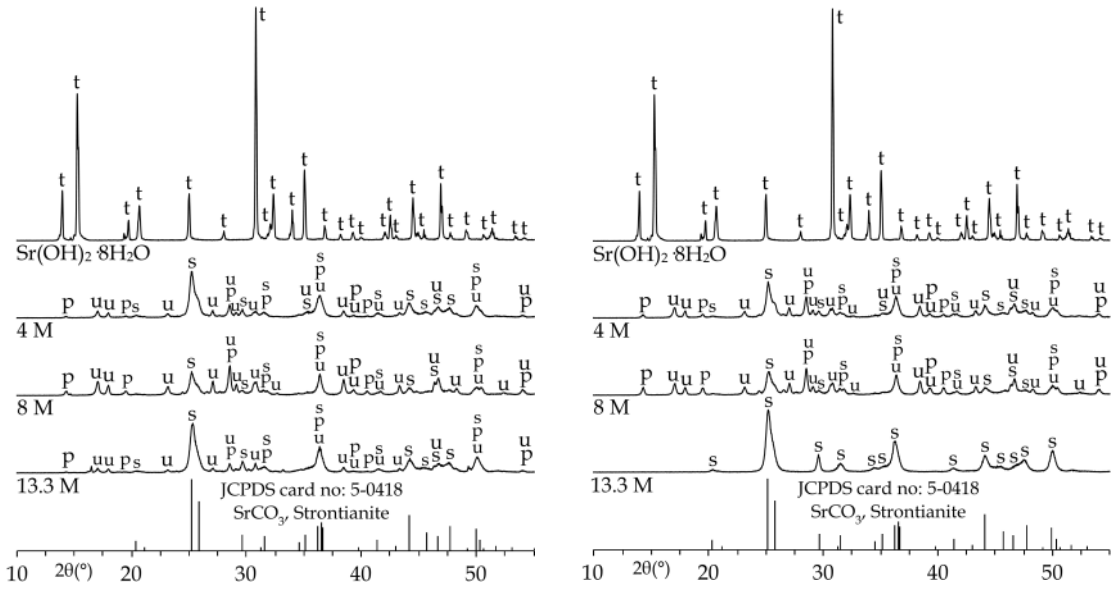

Fig. 4. XRD patterns of $Sr(OH)_2 \cdot 8H_2O$ and its converted solids obtained after conversion in indicated pregnant solutions ($Sr:CO_3^{2-}$ mole ratios; left 1:1 and right 1:2) (t:$Sr(OH)_2 \cdot 8H_2O$, p:$Sr(OH)_2 \cdot H_2O$, u:$Sr(OH)_2$, s:$SrCO_3$)

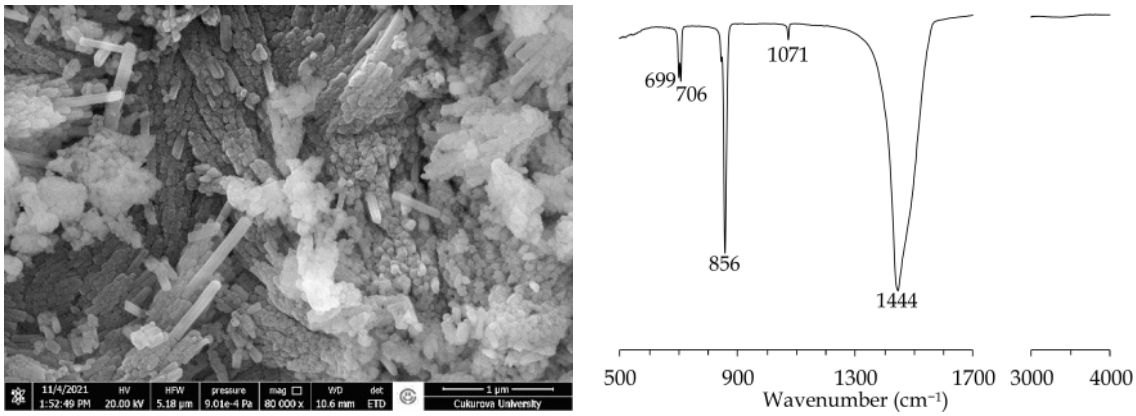

Fig. 5. SEM image (left) and ATR-IR spectrum (right) of converted solid obtained from $Sr(OH)_2 \cdot 8H_2O$

Because single-phase strontium carbonate was only obtained at $Sr:CO_3^{2-}$ mole ratio of 1:2 for the strontium containing $Sr(OH)_2 \cdot 8H_2O$ solid, the comparative direct conversion experiments were performed on reagent grade $SrSO_4$ and natural $SrSO_4$ (celestine) solids only at $Sr:CO_3^{2-}$ mole ratio of 1:2. According to the XRD patterns of $SrSO_4$, celestine and their converted solids obtained by direct conversion at $Sr:CO_3^{2-}$ mole ratio 1:2 in 4 M, 8 M and 13.3 M pregnant solutions, it can be said that both solid sulfates did not convert completely to strontium carbonate, as easily observed by the remaining XRD peaks of unreacted strontium sulfate, i.e. at 2θ=23.59, 27.05, 28.05, 30.06 and 32.74° (JCPDS card no: 5-0593), in the patterns of converted solids (Fig. 6). Although complete conversion of strontium sulfate to its carbonate according to Eq. (1) was expected, it did not occur readily as for the calcium-containing solids, probably due to the lower (room) temperature applied and the possible kinetic restriction, i.e. formation of a porous product layer, mentioned in the literature studies (Carrillo et al., 1995; Castillejos et al., 1996).

Zoraga and Kahruman (2014) and Zoraga et al. (2016) investigated the direct conversion of celestine to strontium carbonate in aqueous solutions of ammonium carbonate (the solutions contained different amounts of NH_4^+, CO_3^{2-}, HCO_3^-, H_2CO_3 and NH_3 species) with dissolved CO_3^{2-} concentrations varying between 0.0089-0.133 mol/L and pH of approximately 8.9, and they observed that conversion of celestine to strontium carbonate decreased with increasing CO_3^{2-} concentration. On the other hand, Hizli et al. (2017) used aqueous ammonium carbonate solutions having stoichiometric amounts of carbonate and they reported that ammonium carbonate was not effective alone for the conversion and

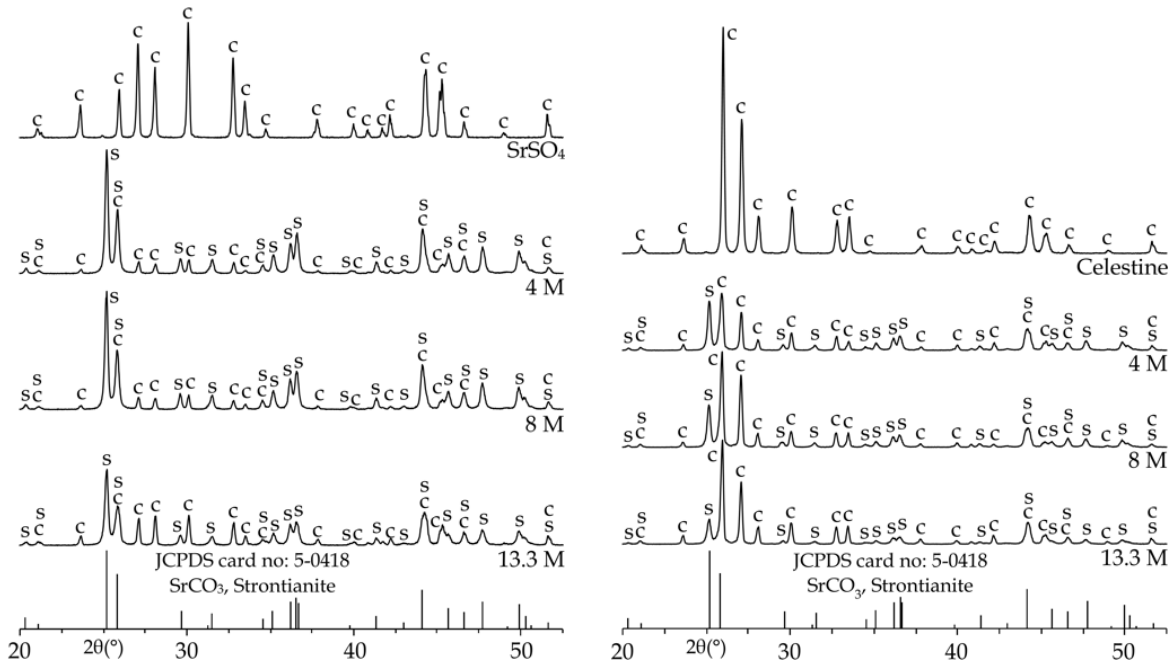

Fig. 6. XRD patterns of (left) reagent grade $SrSO_4$, (right) natural $SrSO_4$ (celestine) and their converted solids obtained after conversion in indicated pregnant solutions ($Sr:CO_3^{2-}$ mole ratio: 1:2) (c:$SrSO_4$, s:$SrCO_3$)

extra additions of ammonia to the solutions were needed for the complete conversion of celestine to strontium carbonate. In the above-mentioned studies, the conversion ratio of celestine to strontium carbonate was observed to increase with increasing conversion time. In this study, where dissolved CO_3^{2-} concentrations and pH varied between 0.40-1.38 mol/L and 11.6-12.9, respectively, and the pregnant solutions contained dominantly zinc ammine complex, the converted solid having lowest unreacted strontium sulfate content was obtained in 4 M pregnant solution at $Sr:CO_3^{2-}$ mole ratio of 1:2.In order to reveal the possible effects of various dissolved zinc complexes on the conversion behavior of celestine to strontium carbonate in ammonia or sodium hydroxide solutions, a further detailed study should be performed in the future using synthetic solutions having different CO_3^{2-} concentrations and pH values.

As in the study of Ehsani and Obut (2019), in which reagent grade $SrSO_4$ completely converted to $SrCO_3$ in a dissolved carbonate-containing pregnant solution formed after leaching of a smithsonite ore sample in 3 M NaOH solution at $Sr:CO_3^{2-}$ mole ratio of 1:2 for conversion time of two hours, achieving the complete conversion from strontium sulfate to strontium carbonate, possibly by increasing the conversion time, may also provide a new and different commercial production method for strontium carbonate during the processing of smithsonite ores by direct ammonia leaching. On the other hand, it was observed that no strontium zincate phase, such as $SrZn(OH)_4 \cdot H_2O$ (Stahl and Jacobs, 1997a), formed during the conversion experiments performed by using $SrSO_4$.

Because generally more pure or single-phase converted solids obtained in 4 M pregnant solution at alkaline earth metal to dissolved carbonate mole ratio of 1:2, the direct conversion behaviors of barium and magnesium-containing solids were investigated under these conditions. The XRD patterns of $Ba(OH)_2 \cdot 8H_2O$, $BaSO_4$ and their converted solids (Fig. 7) obtained by direct conversion at $Ba:CO_3^{2-}$ mole ratio of 1:2 in 4 M pregnant solution showed that barium hydroxide octahydrate completely converted to barium carbonate as observed by the total disappearance of $Ba(OH)_2 \cdot 8H_2O$ peaks, i.e. at 2θ=14.81, 15.15 and 20.59° (JCPDS card no: 26-0155), in XRD pattern of the converted solid, which was single-phase barium carbonate, as identified by the peaks observed mainly at 2θ values of 23.92, 34.15 and 42.04° (Witherite, JCPDS card no: 5-0378). The pattern of reagent grade $Ba(OH)_2 \cdot 8H_2O$ contained some XRD peaks of $BaCO_3$, possibly as a result of interaction with carbon dioxide present in the air (Zhang and Saito, 1997). The complete conversion of water-soluble $Ba(OH)_2 \cdot 8H_2O$ ($3.76^{20°C}$ g/100 g H_2O; Patnaik, 2003) to insoluble $BaCO_3$ ($0.0025^{25°C}$ g/100 mL H_2O; Patnaik, 2003) was predicted because of

the negative free energy change of the theoretical conversion reaction (Eq. (5)) (Benson and Teague, 1980; Barin, 1995; Free, 2013). The obtained barium carbonate may be used for removal of sulfate from various aqueous streams and may also find uses in production of various glass and ceramic products (Kresse et al., 2012). On the contrary, as expected, $BaSO_4$ did not convert to $BaCO_3$ (see Fig. 7) because of the lower solubility product constant of $BaSO_4$ (Table 1) and the positive free energy change of Eq. (6) (Barin, 1995; Free, 2013). In addition, the possible conversion of barium sulfate to barium hydroxide (Eq. (7)) also did not occur. As seen from Fig. 7, however, any kind of barium zincate phase, such as $BaZn_2(OH)_6 \cdot 5H_2O$ (Stahl and Jacobs, 1997b), did not form during the conversion experiments performed by using either $Ba(OH)_2 \cdot 8H_2O$ or $BaSO_4$.

$$Ba(OH)_2 \cdot 8H_2O_{(s)} + CO_3^{2-}{}_{(aq)} \leftrightarrow BaCO_{3(s)} + 2OH^-_{(aq)} + 8H_2O_{(l)} \quad (\Delta G^0 = -28.3 \text{ kJ/mol}) \tag{5}$$

$$BaSO_{4(s)} + CO_3^{2-}{}_{(aq)} \leftrightarrow BaCO_{3(s)} + SO_4^{2-}{}_{(aq)} \quad (\Delta G^0 = 7.7 \text{ kJ/mol}) \tag{6}$$

$$BaSO_{4(s)} + 2OH^-_{(aq)} \leftrightarrow Ba(OH)_{2(s)} + SO_4^{2-}{}_{(aq)} \quad (\Delta G^0 = 72.6 \text{ kJ/mol}) \tag{7}$$

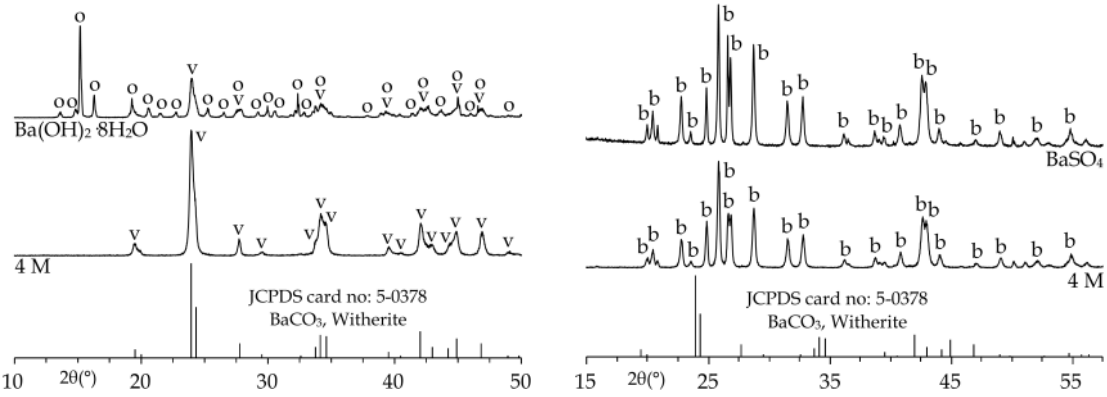

Fig. 7. XRD patterns of $Ba(OH)_2 \cdot 8H_2O$ (left), $BaSO_4$ (right) and their converted solids obtained after conversion in 4 M pregnant solution at $Ba:CO_3^{2-}$ mole ratio of 1:2 (b:$BaSO_4$, o:$Ba(OH)_2 \cdot 8H_2O$, v:$BaCO_3$)

The SEM image of the single-phase converted solid obtained from $Ba(OH)_2 \cdot 8H_2O$ (Fig. 8) displayed that all converted barium carbonate particles had rod-like morphology, as for different barium carbonates prepared in the previous literature studies (Xu and Xue, 2006; Shamsipur et al., 2013; Shahid et al., 2018). It could also be seen from Fig. 8 that the converted solid had adsorptions at 1417 cm^{-1}, 1060 cm^{-1}, 856 cm^{-1} and 693 cm^{-1}, respectively, due to asymmetric stretching, symmetric stretching, out-of-plane bending and planar bending of carbonate groups in the structure of barium carbonate solid (Adler and Kerr, 1963).

The XRD patterns of $Mg(OH)_2$, $MgSO_4 \cdot 7H_2O$ and their converted solids (Fig. 9) obtained by direct conversion at $Mg:CO_3^{2-}$ mole ratio of 1:2 in 4 M pregnant solution indicated that both magnesium-containing solids did not convert to magnesium carbonate under the studied experimental conditions.

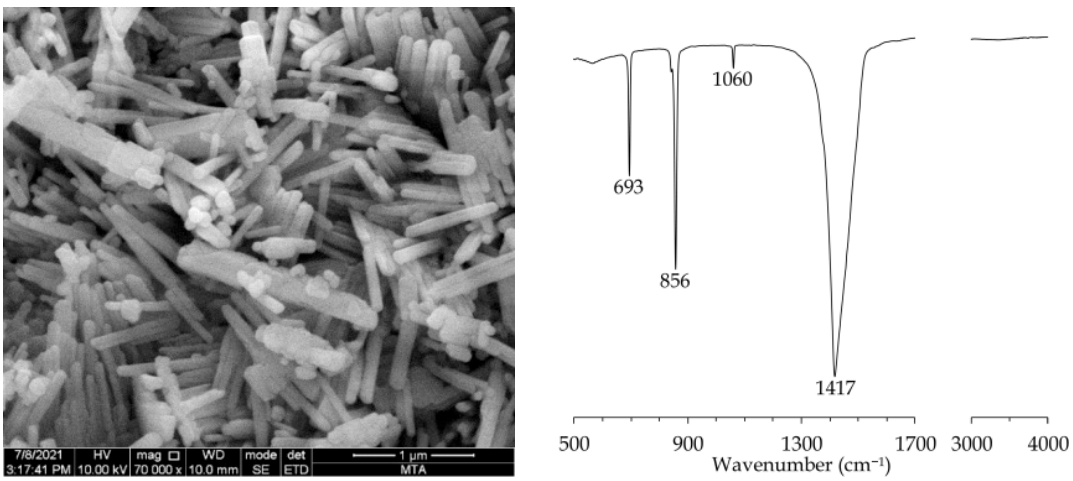

Fig. 8. SEM image (left) and ATR-IR spectrum (right) of converted solid obtained from $Ba(OH)_2 \cdot 8H_2O$

Because of the lower solubility product constant of $Mg(OH)_2$ in comparison to $MgCO_3$ (Table 1), the hydroxide did not convert to its carbonate form (see Eq. (8)). On the other hand, the magnesium sulfate heptahydrate (including some $MgSO_4 \cdot 6H_2O$ as impurity), which is freely water-soluble ($71.0^{20°C}$ g/100 mL H_2O; Patnaik, 2003), converted dominantly to a magnesium zinc carbonate hydroxide hydrate ($Mg_5Zn_3(CO_3)_2(OH)_{12} \cdot H_2O$) containing solid with some unidentified impurity phase(s) (Fig. 9), in place of the expected magnesium carbonate (Eq. (9)) and magnesium hydroxide (Eq. (10)) phases. In the literature, an unnamed zinc-magnesium-carbonate-hydroxide mineral from Sterling Hill (New Jersey, USA) was first described by Dunn (1986) with main XRD peaks observed at 2θ=11.85, 33.26 and 58.86° (JCPDS card no: 41-1436). In this study, the main XRD peaks of tentatively identified magnesium zinc carbonate hydroxide hydrate were observed at 2θ values of 11.84, 33.16 and 59.14°. In addition, the converted solid effervesced vigorously when interacted with a 10% hydrochloric acid solution, as also experienced by Dunn (1986). On the other hand, in this study, no crystalline magnesium zincate phase was observed to form, as indicated by Ropp (2013), during the conversion experiments performed using magnesium hydroxide and magnesium sulfate heptahydrate solids. Besides, separate crystalline magnesium (i.e., $(NH_4)_2Mg(CO_3)_2 \cdot 4H_2O$, Erdos et al., 1979) and zinc (i.e., $Zn(NH_3)CO_3$, Ehsani et al., 2021) containing phases that could be prepared in dissolved carbonate-containing ammoniacal media also were not observed to form during the conversion experiments performed by using either $Mg(OH)_2$ or $MgSO_4 \cdot 7H_2O$.

The DTA curve (Fig. 10) of converted solid obtained from $MgSO_4 \cdot 7H_2O$ contained, other than low-temperature endotherm near 105°C, only one strong endotherm centered at 390.8°C, which was found to be related with the decomposition of $Mg_5Zn_3(CO_3)_2(OH)_{12} \cdot H_2O$ phase into its corresponding oxides (Fig. 11). The peak temperature of the endotherm lied between decomposition peak temperatures of synthetic magnesium (for $Mg_5(CO_3)_4(OH)_2 \cdot 4H_2O$, between 420-475°C) and zinc (for $Zn_5(CO_3)_2(OH)_6$, between 245-270°C) hydroxycarbonates (Jambor, 1964; Koga and Yamane, 2008; Vagvolgyi et al., 2008a,b; Frost et al., 2009; Bhattacharjya et al., 2012; Yamamoto et al., 2021). As also seen from Fig. 10, dominantly $Mg_5Zn_3(CO_3)_2(OH)_{12} \cdot H_2O$ containing converted solid had a strong split band with peaks at 1392-1518 cm^{-1} and a weak band at 858 cm^{-1}, both probably be related to asymmetric stretching and out-of-plane bending of the carbonate groups, respectively. The absorption bands centered at 1043 cm^{-1}, 1642 cm^{-1} and 3300 cm^{-1} may be related to hydroxyl and water contents in the converted solid. The very strong band observed at 563 cm^{-1} was tentatively assigned to the vibrations between metal (magnesium/zinc)-oxygen bonds present in the structure of converted solid (Remazeilles and Refait, 2009; Winiarski et al., 2018).

$$Mg(OH)_{2(s)} + CO_3^{2-}{}_{(aq)} \leftrightarrow MgCO_{3(s)} + 2OH^-{}_{(aq)} \quad (\Delta G^0 = 34.7 \text{ kJ/mol}) \tag{8}$$

$$MgSO_4 \cdot 7H_2O_{(s)} + CO_3^{2-}{}_{(aq)} \leftrightarrow MgCO_{3(s)} + SO_4^{2-}{}_{(aq)} + 7H_2O_{(l)} \quad (\Delta G^0 = -17.7 \text{ kJ/mol}) \tag{9}$$

$$MgSO_4 \cdot 7H_2O_{(s)} + 2OH^-{}_{(aq)} \leftrightarrow Mg(OH)_{2(s)} + SO_4^{2-}{}_{(aq)} + 7H_2O_{(l)} \quad (\Delta G^0 = -52.4 \text{ kJ/mol}) \tag{10}$$

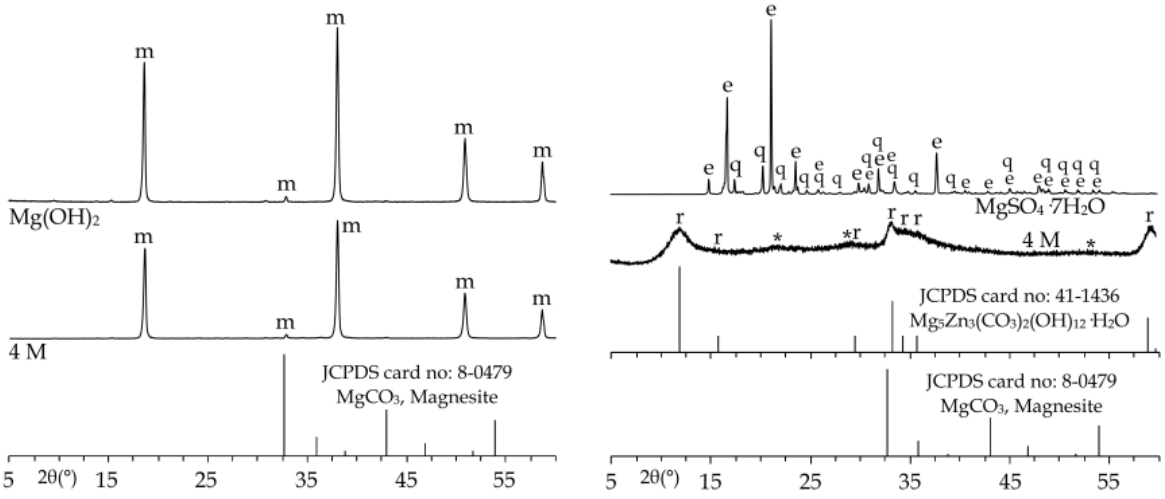

Fig. 9. XRD patterns of $Mg(OH)_2$ (left), $MgSO_4 \cdot 7H_2O$ (right) and their converted solids obtained after conversion in 4 M pregnant solution at $Mg:CO_3^{2-}$ mole ratio of 1:2 (e:$MgSO_4 \cdot 7H_2O$, q: $MgSO_4 \cdot 6H_2O$, m:$Mg(OH)_2$, r:$Mg_5Zn_3(CO_3)_2(OH)_{12} \cdot H_2O$, *:unidentified)

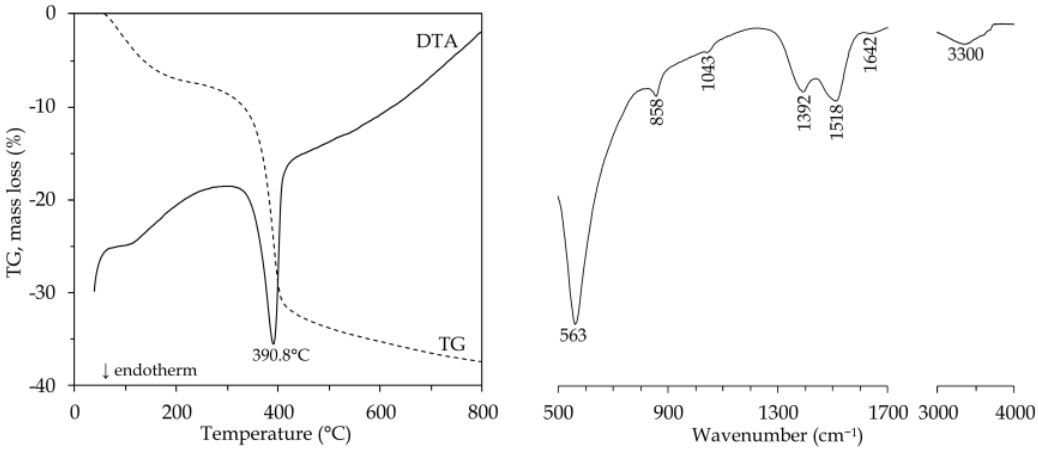

Fig. 10. TG/DTA curves (left) and ATR-IR spectrum (right) of converted solid obtained from $MgSO_4 \cdot 7H_2O$

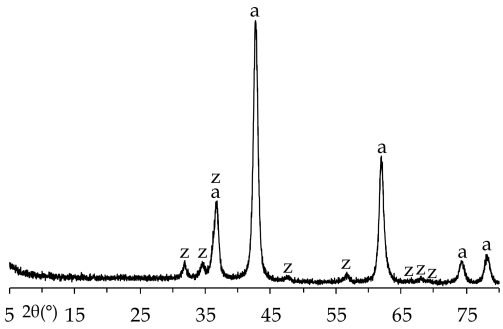

Fig. 11. XRD pattern of the material formed after calcination of the converted solid obtained from $MgSO_4 \cdot 7H_2O$ at 600°C for 1 hour (a: MgO, z: ZnO)

4. Conclusions

The direct conversion behaviors of calcium, strontium, barium and magnesium-containing alkaline earth metal solids to their corresponding carbonates in dissolved carbonate containing pregnant solutions formed after direct leaching of a smithsonite ore sample in aqueous ammonia solutions were investigated to reveal the possible ways for the obtainment of dissolved carbonate component of these solutions as solid alkaline earth metal carbonate by-products. In accord with the solubility product constants, it was observed that the hydroxides of calcium, strontium and barium, and the sulfates of calcium and strontium converted either partially or totally to their corresponding carbonates whereas the hydroxide of magnesium and the sulfate of barium remained unreacted, i.e., did not convert to any other form. Differently, the sulfate of magnesium converted dominantly to a hydrated magnesium zinc carbonate hydroxide containing solid in the dissolved carbonate-containing pregnant solution formed after leaching of smithsonite ore sample in 4 M NH_3 solution. In conclusion, the results of this preliminary study indicated that it may be possible to integrate naturally abundant gypsum and celestine resources, following optimization, into the processing of smithsonite ores by direct ammonia leaching for bulk production of commercial calcium carbonate and strontium carbonate solids, which may find different uses in various industries.

References

ADLER, H.H., KERR, P.F., 1963. *Infrared absorption frequency trends for anhydrous normal carbonates.* Am. Mineral. 48, 124-137.

BARIN, I., 1995. *Thermochemical Data of Pure Substances.* 3rd Edition, VCH, Weinheim.

BENSON, L.V., TEAGUE, L.S., 1980. *A Tabulation of Thermodynamic Data for Chemical Reactions Involving 58 Elements Common to Radioactive Waste Package Systems.* Topical Report for Rockwell International, 97 p.

BHATTACHARJYA, D., SELVAMANI, T., MUKHOPADHYAY, I., 2012. *Thermal decomposition of hydromagnesite-Effect of morphology on the kinetic parameters.* J. Therm. Anal. Calorim. 107, 439-445.

BINGOL, D., AYDOGAN, S., BOZBAS, S.K., 2012. *Production of $SrCO_3$ and $(NH_4)_2SO_4$ by the dry mechanochemical processing of celestite.* J. Ind. Eng. Chem. 18, 834-838.

CARRILLO, F.R.P., URIBE, A.S., CASTILLEJOS, A.H.E., 1995. *A laboratory study of the leaching of celestine in a pachuca tank.* Miner. Eng. 8, 495-509.

CASTILLEJOS, A.H.E., de la CRUZ, F.P. del B., URIBE, A.S., 1996. *The direct conversion of celestite to strontium carbonate in sodium carbonate aqueous media.* Hydrometallurgy 40, 207-222.

CHENG, H., ZHANG, X., SONG, H., 2014. *Morphological investigation of calcium carbonate during ammonification-carbonization process of low concentration calcium solution.* J. Nanomater. Article ID 503696, 7 p.

DING, Z., CHEN, Q., YIN, Z., LIU, K., 2013. *Predominance diagrams for Zn(II)-NH_3-Cl^--H_2O system*. Trans. Nonferrous Met. Soc. China.23, 832-840.

DUNN, P.J., 1986. *A new zinc magnesium carbonate and data for other unnamed species from Franklin and Sterling Hill, New Jersey.* Journal of the Franklin-Ogdensburg Mineralogical Society 27, 25-26.

EHSANI, A., EHSANI, I., OBUT, A., 2021. *Preparation of different zinc compounds from a smithsonite ore through ammonia leaching and subsequent heat treatment.* Physicochem. Probl. Mi. 57, 96-106.

EHSANI, I., OBUT, A., 2019. *Conversion behaviours of Sr- and Ca-containing solids in dissolved carbonate containing alkaline pregnant zinc leaching solutions.* Miner. Eng. 135, 9-12.

ENGHAG, P., 2004. *Encyclopedia of the Elements.* WILEY-VCH, Weinheim.

ERDEMOGLU, M., AYDOGAN, S., CANBAZOGLU, M., 2007. *A kinetic study on the conversion of celestite ($SrSO_4$) to $SrCO_3$ by mechanochemical processing.* Hydrometallurgy 86, 1-5.

ERDOS, E., ALTORFER, H., WITT, J., 1979. *Crystal data for ammonium magnesium carbonate tetrahydrate $[(NH_4)_2Mg(CO_3)_2 \cdot 4H_2O]$.* J. Appl. Cryst. 12, 611.

FREE, M.L., 2013. *Hydrometallurgy: Fundamentals and Applications.* John Wiley & Sons, New Jersey.

FRENAY, J., 1985. *Leaching of oxidized zinc ores in various media.* Hydrometallurgy 15, 243-253.

FROST, R.L., HALES, M.C., MARTENS, W.N., 2009. *Thermogravimetric analysis of selected group (II) carbonate minerals-Implication for the geosequestration of greenhouse gases.* J. Therm. Anal. Calorim. 95, 999-1005.

HARVEY, T.G., 2006. *The hydrometallurgical extraction of zinc by ammonium carbonate: A review of the Schnabel process.* Miner. Process. Extr. Metall. Rev. 27, 231-279.

HIZLI, I.G., BILEN, A., SEZER, R., ERTURK, S., ARSLAN, C., 2017. *Production of strontianite from celestite ore in carbonate media.* Proceedings of the 3rd Pan American Materials Congress, pp. 607-613.

ICIN, K., OZTURK, S., SUNBUL, S.E., 2021. *Investigation and characterization of high purity and nano-sized $SrCO_3$ production by mechanochemical synthesis process.* Ceram. Int. 47, 33897-33911.

JAMBOR, J.L., 1964. *Studies of basic copper and zinc carbonates: I - Synthetic zinc carbonates and their relationship to hydrozincite.* Can. Mineral. 8, 92-108.

JIMOH, O.A., ARIFFIN, K.S., HUSSIN, H.B., TEMITOPE, A.E., 2018. *Synthesis of precipitated calcium carbonate: a review.* Carbonate. Evaporite. 33, 331-346.

KOGA, N., YAMANE, Y., 2008. *Effect of mechanical grinding on the reaction pathway and kinetics of the thermal decomposition of hydro-magnesite.* J. Therm. Anal. Calorim. 93, 963-971.

KRALJ, D., KONTREC, J., BRECEVIC, L., FALINI, G., NOTHIG-LASLO, V., 2004. *Effect of inorganic anions on the morphology and structure of magnesium calcite.* Chem.-Eur. J. 10, 1647-1656.

KRESSE, R., BAUDIS, U., JAGER, P., RIECHERS, H.H., WAGNER, H., WINKLER, J., WOLF, H.U., 2012. *Barium and barium compounds.* Ullmann's Encyclopedia of Industrial Chemistry, WILEY-VCH, Weinheim.

LI, L., LIN, R., TONG, Z., FENG, Q., 2012. *Facile synthesis of $SrCO_3$ nanostructures in methanol/water solution without additives.* Nanoscale Res. Lett. 7, 305.

LI, S., LI, H., CHEN, W., PENG, J., MA, A., YIN, S., ZHANG, L., YANG, K., 2018. *Ammonia leaching of zinc from low-grade oxide zinc ores using the enhancement of the microwave irradiation.* Int. J. Chem. React. Eng. 16, 1-9.

LIDE, D.R. (Editor-in-Chief), 2010. *CRC Handbook of Chemistry and Physics*. 90th Edition, CRC Press, Florida.

LIU, Q., MA, Y., DUAN, X., ZHOU, Y., LIU, X., PEI, C., 2014. *Controlled crystallization of lamellar calcium carbonate crystals induced by solution of sticky rice polysaccharide (from Oryza sativa).* CrystEngComm 16, 11042-11049.

MTA, 2021. *Mineral and energy resources of Sivas province.* General Directorate of Mineral Exploration and Research, https://www.mta.gov.tr/v3.0/sayfalar/bilgi-merkezi/maden_potansiyel_2010/sivas_madenler.pdf, accessed 15 August 2021 (in Turkish).

OBUT, A., BALAZ, P., GIRGIN, I., 2006. *Direct mechanochemical conversion of celestite to $SrCO_3$.* Miner. Eng. 19, 1185-1190.

PATNAIK, P., 2003. *Handbook of Inorganic Chemicals*. McGraw-Hill, New York.

PHIPPS, J.S., 2014. *Engineering minerals for performance applications: an industrial perspective.* Clay Miner. 49, 1-16.

PULLAR, R.C., 2012. *Hexagonal ferrites: A review of the synthesis, properties and applications of hexaferrite ceramics.* Prog. Mater. Sci. 57, 1191-1334.

REMAZEILLES, C., REFAIT, P., 2009. *Fe(II) hydroxycarbonate $Fe_2(OH)_2CO_3$ (chukanovite) as iron corrosion product: Synthesis and study by Fourier Transform Infrared Spectroscopy.* Polyhedron 28, 749-756.

ROPP, R.C., 2013. *Encyclopedia of the Alkaline Earth Compounds.* Elsevier, Amsterdam.

SETOUDEH, N., WELHAM, N.J., AZAMI, S.M., 2010. *Dry mechanochemical conversion of $SrSO_4$ to $SrCO_3$.* J. Alloy. Compd. 492, 389-391.

SEZER, R., ARSLAN, C., 2019. *Mechano-chemical conversion of celestite in highly concentrated sodium carbonate media. Physicochem.* Probl. Mi. 55, 324-335.

SHAHID, T., ARFAN, M., ZEB, A., BIBI, T., KHAN, T.M., 2018. *Preparation and physical properties of functional barium carbonate nanostructures by a facile composite-hydroxide-mediated route.* Nanomater. Nanotechnol. 8, 1-8.

SHAMSIPUR, M., POURMORTAZAVI, S.M., HAJIMIRSADEGHI, S.S., ROUSHANI, M., 2013. *Applying Taguchi robust design to the optimization of synthesis of barium carbonate nanorods via direct precipitation.* Colloid. Surface. A 423, 35-41.

SINGERLING, S.A., 2017. *Strontium - Advance Release*. U.S. Geological Survey Minerals Yearbook, 7 p.

STAHL, R., JACOBS, H., 1997a. *Zur kristallstruktur von $SrZn(OH)_4 \cdot H_2O$.* Z. Anorg. Allg. Chem. 623, 1273-1276.

STAHL, R., JACOBS, H., 1997b. *Synthese und kristallstruktur von $BaZn_2(OH)_6 \cdot 5H_2O$.* Z. Anorg. Allg. Chem. 623, 423-428.

SUAREZ-ORDUNA, R., RENDON-ANGELES, J.C., LOPEZ-CUEVAS, J., YANAGISAWA, K., 2004. *The conversion of mineral celestite to strontianite under alkaline hydrothermal conditions.* J. Phys.-Condens. Mat. 16, S1331-S1344.

SUAREZ-ORDUNA, R., RENDON-ANGELES, J.C., YANAGISAWA, K., 2007. *Kinetic study of the conversion of mineral celestite to strontianite under alkaline hydrothermal conditions.* Int. J. Miner. Process. 83, 12-18.

THENEPALLI, T., JUN, A.Y., HAN, C., RAMAKRISHNA, C., AHN, J.W., 2015. *A strategy of precipitated calcium carbonate ($CaCO_3$) fillers for enhancing the mechanical properties of polypropylene polymers.* Korean J. Chem. Eng. 32, 1009-1022.

VAGVOLGYI, V., FROST, R.L., HALES, M., LOCKE, A., KRISTOF, J., HORVATH, E., 2008a. *Controlled rate thermal analysis of hydromagnesite.* J. Therm. Anal. Calorim. 92, 893-897.

VAGVOLGYI, V., HALES, M., MARTENS, W., KRISTOF, J., HORVATH, E., FROST, R.L., 2008b. *Dynamic and controlled rate thermal analysis of hydrozincite and smithsonite.* J. Therm. Anal. Calorim. 92, 911-916.

WANG, Y.-M., WAINWRIGHT, G., 1986. *Formation and decomposition kinetic studies of calcium zincate in 20 w/o KOH.* J. Electrochem. Soc. 133, 1869-1872.

WINIARSKI, J., TYLUS, W., WINIARSKA, K., SZCZYGIEL, I., SZCZYGIEL, B., 2018. *XPS and FT-IR characterization of selected synthetic corrosion products of zinc expected in neutral environment containing chloride ions.* J. Spectrosc. Article ID 2079278, 14 p.

XU, J., XUE, D., 2006. *Chemical synthesis of $BaCO_3$ with a hexagonal pencil-like morphology.* J. Phys. Chem. Solids 67, 1427-1431.

YAMAMOTO, G., KYONO, A., SANO, Y., MATSUSHITA, Y., YONEDA, Y., 2021. *In situ and ex situ studies on thermal decomposition process of hydromagnesite $Mg_5(CO_3)_4(OH)_2 \cdot 4H_2O$.* J. Therm. Anal. Calorim. 144, 599-609.

YAN, F., ZHANG, X., ASSELIN, E., DUAN, D., LI, Z., 2021. *Preparation of strontium carbonate via celestite leaching in $NaHCO_3$ using two interconnected reactors*. Hydrometallurgy 204, 105729.

ZHANG, W., YU, Y., YI, Z., 2017. *Controllable synthesis of $SrCO_3$ with different morphologies and their co-catalytic activities for photocatalytic oxidation of hydrocarbon gases over TiO_2.* J. Mater. Sci. 52, 5106-5116.

ZHANG, Q., SAITO, F., 1997. *Non-thermal production of barium carbonate from barite by means of mechanochemical treatment.* J. Chem. Eng. Jpn. 30, 724-727.

ZHU, A.L., DUCH, D., ROBERTS, G.A., LI, S.X.X., WANG, H., DUCH, K., BAE, E., JUNG, K.S., WILKINSON, D., KULINICH, S.A., 2015. *Increasing the electrolyte capacity of alkaline Zn-air fuel cells by scavenging zincate with $Ca(OH)_2$.* ChemElectroChem 2015, 134-142.

ZORAGA, M., KAHRUMAN, C., 2014. *Kinetics of conversion of celestite to strontium carbonate in solutions containing carbonate, bicarbonate and ammonium ions, and dissolved ammonia.* J. Serb. Chem. Soc. 79, 345-359.

ZORAGA, M., KAHRUMAN, C., YUSUFOGLU, I., 2016. *Conversion kinetics of $SrSO_4$ to $SrCO_3$ in solutions obtained by dissolving/hydrolyzing of equimolar amounts of NH_4HCO_3 and NH_4COONH_2.* Hydrometallurgy 163, 120-129.